Journal of Cellular Biochemistry 102:1504–1518 (2007)

Changes in Osteoblast, Chondrocyte, and Adipocyte Lineages Mediate the Bone Anabolic Actions of PTH and Small Molecule GSK-3 Inhibitor

Nalini H. Kulkarni,[1] Tao Wei,[1] Amar Kumar,[1] Ernst R. Dow,[1] Trent R. Stewart,[1] Jianyong Shou,[1] Mathias N'cho,[1] Diane L. Sterchi,[1] Bruce D. Gitter,[1] Richard E. Higgs,[1] David L. Halladay,[1] Thomas A. Engler,[1] T. John Martin,[2] Henry U. Bryant,[1] Yanfei L. Ma,[1] and Jude E. Onyia[1]*

[1]Lilly Research Laboratories, Eli Lilly & Company, Lilly Corporate Center, Indianapolis, Indiana 46285
[2]St. Vincent's Institute of Medical Research, Fitzroy, Victoria 3065, Australia

Abstract Parathyroid hormone (PTH) and glycogen synthase kinase-3 (GSK-3) inhibitor 603281-31-8, administered once daily increased bone formation in vivo. We investigated the molecular mechanisms of the anabolic responses of PTH and 603281-31-8 in rat osteopenia model. Female 6-month-old rats were ovariectomized (Ovx) and permitted to lose bone for 1 month, followed by treatment with PTH (1–38) at 10 μg/kg/day s.c. or 603281-31-8 at 3 mg/kg/day p.o. for 60 days. Twenty-four hours after the last treatment, RNA from distal femur metaphysis was subjected to gene expression analysis. Differentially expressed genes ($P < 0.05$) were subjected to pathway analysis to delineate relevant bio-processes involved in skeletal biology. Genes involved in morphogenesis, cell growth/differentiation, and apoptosis were significantly altered by Ovx and the treatments. Analysis of morphogenesis genes showed an overrepresentation of genes involved in osteogenesis, chondrogenesis, and adipogenesis. A striking finding was that Ovx decreased several markers of osteogenesis/chondrogenesis and increased markers of adipogenesis/lipid metabolism. Treatment with either PTH or the GSK-3 inhibitor reversed these effects, albeit at different levels. Histological analysis confirmed that osteopenia in Ovx animals was associated with three-fold increase in marrow adiposity. PTH and GSK-3 inhibitor restored bone volume, and reversed or normalized marrow adiposity. Ex vivo studies showed that PTH and GSK-3 inhibitor increased the ratio of colony forming marrow stromal progenitors (CFU-fs) that were alkaline phosphatase positive (putative osteoblasts). Our results suggest that the bone anabolic actions of PTH and GSK-3 inhibitor in vivo involve concerted effects on mesenchymal lineages; osteoblasts, chondrocytes, and adipocytes. J. Cell. Biochem. 102: 1504–1518, 2007.

Key words: ovariectomy; GSK-3 inhibitor; parathyroid hormone; gene arrays; adipogenesis; osteogenesis; chondrogenesis

Parathyroid hormone (PTH), given intermittently stimulates net gain in bone mass in humans and experimental animals [Hock, 2001; Neer et al., 2001; Rosen and Bilezikian, 2001]. Anabolic response of bone to PTH has been largely explained by an increase in osteoblast differentiation, activity, survival, and recruitment of committed precursors and lining cells to active osteoblasts [Dobnig and Turner, 1995; Onyia et al., 1995; 1997; Bellido et al., 2003]. PTH binding to its receptor on the osteoblast or osteoblast lineage cells results in the activation of cAMP/PKA, phospholipase C (PLC), or D (PLD) and PKC signaling pathways culminating in the expression of downstream genes to mediate biologic activity [Civitelli et al., 1988; Babich et al., 1991; Scott et al., 1992; Rixon et al., 1994; Miles et al., 2000a,b, 2002; Radeff et al., 2004; Onyia et al., 2005]. The cAMP/PKA pathway has been the most extensively studied and is likely the predominant PTH signaling pathway in osteoblasts. Previously, we and others have shown that PTH increased the levels of β-catenin, a major component of the

This article contains supplementary material, which may be viewed at the Journal of Cellular Biochemistry website at http://www.interscience.wiley.com/jpages/0730-2312/suppmat/index.html.

*Correspondence to: Jude E. Onyia, Integrative Biology, Lilly Corporate Center GL54, Indianapolis, IN 46285.
E-mail: jeo@lilly.com

Received 11 September 2006; Accepted 14 March 2007
DOI 10.1002/jcb.21374

Wnt pathway [Kulkarni et al., 2005; Tobimatsu et al., 2006]. However, the precise role and contribution of the Wnt signaling pathway to the bone anabolic action of PTH remains to be elucidated.

The canonical Wnt signaling pathway is crucial for the specification of cell fates, regulation of cell growth, differentiation and apoptosis [Wodarz and Nusse, 1998; Uusitalo et al., 1999; Westendorf et al., 2004]. Wnt ligands are secreted lipid-modified glycoproteins that signal through a receptor complex comprised of a member of the family of seven transmembrane domain receptors known as Frizzleds, and the co-receptor lipoprotein-receptor-related proteins 5 or 6 (LRP5/6) [Yang-Snyder et al., 1996; He et al., 1997; Slusarski et al., 1997; Wang et al., 1997; Hsieh et al., 1999; Pinson et al., 2000; Mao et al., 2001a,b]. The resulting signal is propagated and integrated through a downstream key signaling serine/threonine kinase known as glycogen synthase kinase-3β (GSK-3β). Genetic and biochemical studies have implicated the Wnt signaling pathway as an important regulator of bone mass. Activating mutations in LRP5 have been shown to result in a high bone mass phenotype associated with increased bone formation and no other obvious abnormalities in humans and animals, whereas inactivating mutations in LRP5 result in osteoporosis-pseudoglioma syndrome (OPPG) [Gong et al., 2001; Boyden et al., 2002; Little et al., 2002; Babij et al., 2003; Wesenbeeck et al., 2003]. In mice, targeted disruption of LRP5 and/or LRP 6, or over-expression of DKK-1, a Wnt inhibitor lead to a low bone mass phenotype due to a decrease in bone formation [Kato et al., 2002; Guo et al., 2004; Holmen et al., 2004]. Conversely, over-expression of LRP5 transgene bearing the activating mutation or knockout of inhibitors DKK-1, or sFRP-1 resulted in a high bone mass phenotype explained by an increase in bone formation [Babij et al., 2003; Wang et al., 2005]. In addition to the focus on the osteoblast lineage and formation effects of Wnt signaling, two recent studies of genetically engineered mice showed a profound effect of β-catenin on resorption via stimulation of production of OPG, a major inhibitor of osteoclast differentiation [Glass et al., 2005; Holmen et al., 2005]. Similarly, patients with autosomal dominant osteopetrosis type I (ADOI) due to T253I mutation in LRP5, manifest an osteopetrotic phenotype, with lower numbers of osteoclasts in vivo [Bollerslev et al., 1989, 1993], but show no increase in bone formation markers [Bollerslev et al., 1998]. Thus, different outcomes on osteoblast and/or osteoclast function may depend on the nature and location of mutations in LRP5, or perhaps on the mode or nature of activation of Wnt signaling.

Recently, we have shown that an orally active, potent, and selective small molecule GSK-3 (α/β) dual inhibitor (603281-31-8) that stimulates Wnt/β-catenin signaling pathway increases osteoblast differentiation, markers of bone formation, bone mass, and strength in osteopenic rats (ovariectomized, Ovx) in vivo [Kulkarni et al., 2006]. 603281-31-8 effects were driven by a primary and robust increase in de novo bone formation, with a subtle effect on resorption. The anabolic effects have also been replicated in studies using LiCl, a less potent and specific inhibitor of GSK-3 [Lacroix et al., 2005]. Thus, pharmacological manipulation of the Wnt signaling pathway (perhaps via inhibition of GSK-3) remains a viable strategy for increasing bone mass.

To better understand the molecular basis of bone formation and the role of Wnt signaling, we investigated the anabolic actions of PTH and 603281-31-8 in a rat osteopenia model using whole genome array analysis and pathway mapping. We demonstrate that ovariectomy altered markers of osteogenesis, chondrogenesis, and adipogenesis, and treatment with PTH or 603281-31-8 reversed these effects, albeit at different levels. Additionally, we demonstrate that ex vivo PTH and 603281-31-8 increased the ratio of putative osteoblasts (ALP^+CFU-f colonies) through differential effects on bone marrow progenitors.

EXPERIMENTAL PROCEDURES

Biochemicals

Synthetic human PTH (1-38) obtained from (Bachem, Torrence, CA) was prepared in a vehicle of acidified saline containing 2% heat-inactivated rat serum. GSK-3 α/β dual inhibitor, 603281-31-8 was synthesized at the Lilly Research Laboratories (Indianapolis, IN) as previously described [Engler et al., 2004].

Animals and Dosing Regimen

Six-month-old virgin Sprague–Dawley female rats (Harlan Industries, Indianapolis,

IN) weighing approximately 220 g were maintained on a 12-h light/12-h dark cycle at 22°C with ad libitum access to food (TD 89222 with 0.5% Ca and 0.4% P, Tekdad, Madison, WI) and water. Bilateral ovariectomies (Ovx) were performed on the rats except for the Sham-operated controls, and then randomized into treatment groups of eight rats in each group. Ovx rats were permitted to lose bone for 1 month to establish osteopenia before the initiation of treatments. PTH(1-38) was administered s.c., at a dose of 10 μg/kg/day or GSK-3 inhibitor 3 mg/kg/day was given to the Ovx rats via oral gavage for 2 months. 603281-31-8 (Eli Lilly and Company) was prepared in 1% CMC/0.25% Tween 80 vehicle. Animals were weighed every 2 weeks and the dosing volumes were adjusted accordingly. The protocols were approved by the Animal Care Committee of Lilly Research Labs to ensure compliance with NIH guidelines. Twenty-four hours after the last dosing, the animals were euthanized by CO_2 inhalation. From the left femur, the distal epiphysis including the growth plate was removed and a subjacent 3 mm band of the metaphyseal primary spongiosa was resected for mRNA analysis [Onyia et al., 1995; McClelland et al., 1998]. The left tibia was excised fixed in buffered-formaldehyde, decalcified and embedded in paraffin and used for histological analysis for adipocytes and fat. For validation of gene expression changes with short-term PTH treatment, 6-month-old virgin Sprague–Dawley female rats were injected s.c., with 80 μg/kg/day for 7 days and were sacrificed 24 h after last dose. Vehicle controls were administered saline once daily for 7 days.

RNA Isolation

At the end of each treatment, tissue samples were removed from the animals, snap frozen in liquid nitrogen as individual samples (8 animals/group). Total RNA was isolated from the metaphyseal primary spongiosa of rats treated with vehicle, PTH, or 603281-31-8 as previously described [Onyia et al., 1995; McClelland et al., 1998] by homogenization in Ultraspec-II™ reagent (Biotecx, Houston, TX) using an LS 10-35 Polytron homogenizer (Brinkmann Instruments, Westbury, NY) as recommended by the manufacturer. RNA was quantified by measuring the absorbance at 260 nm and the quality of the RNA samples were assessed by agarose gel electrophoresis for the integrity of 18S and 28S ribosomal RNA bands and also by the 260/280 nm absorbance ratio.

Microarray Analysis

Total RNA from distal femur metaphysis was amplified and hybridized onto rat RAE230V2 GeneChips according to the protocols recommended by Affymetrix (Santa Clara, CA); 31042 probe sets on the arrays were analyzed. RNA was purified through RNeasy columns (Qiagen, Valencia, CA) and concentrated. An aliquot of the cleaned total RNA was tested for quality with the Agilent 2100 Bioanalyzer as per manufacturer's protocol (Agilent, Palo Alto, CA). High quality RNA samples were then subjected to microarray gene expression analysis. Oligo microarray experiments were performed according to standard manufacturer protocol. Briefly, first strand cDNA was reverse transcribed from 5 μg of purified total RNA using a T7-day $(T)_{24}$ primer (Proligo, Boulder, CO) and the SuperScript Double-Stranded cDNA Synthesis Kit (Invitrogen, Carlsbad, CA). After first strand cDNA synthesis, an RNase H mediated second round of amplification was performed with the same kit. Non-essential nucleic acids were removed using a column matrix (Affymetrix Gene Chip Sample Cleanup Module, Santa Clara, CA). In vitro transcription (IVT) of the cDNA to cRNA was performed according to protocol (Enzo Diagnostics, Farmingdale, NY), with T7 RNA polymerase and biotin-labeled ribonucleotides to produce biotinylated cRNA. Purification to remove free NTPs from cRNA products, and hence, ensuring accurate quantitation, was performed using guanidine thiocyanate and spin columns from the Gene Chip Sample Cleanup Module. The cRNA was fragmented to approximately 50 bp size by incubation in buffer at 94°C for 35 min to facilitate hybridization. Hybridization cocktails containing 15 μg fragmented IVT product as well as Affymetrix Eukaryotic controls Oligo B2, for grid alignment, and positive controls spikes (BioB, BioC, BioD, Cre, Dap, Lys, Thr) were added to the Rat Genome 230_2.0 Affymetrix arrays after a prehybridization incubation. The chips were then hybridized for 16 h at 45°C using a rotating (58 rpm) hybridization oven. Following incubation, the cartridges were washed and stained with Streptavidin-R-phycoerythrin conjugate

(SAPE) on an Affymetrix Fluidics Station 450 using an automated protocol (EukGE-WS2v4_450). Single replicate arrays per sample were scanned using the GeneChip Scanner 3000. After image alignment and quality control, raw signal intensities of probesets were determined using Affymetrix microarray suite software (MAS5). Mann–Whitney rank order pairwise comparisons were performed to identify differentially expressed genes by treatment versus non-treated samples.

Functional Analysis of Significant Genes

The differentially expressed probe sets were identified as significant if the comparison had (a) $P < 0.05$; (b) the median signal for all the chips in a group was larger than 250; (c) the comparisons had an absolute fold change greater than 1.2. These genes were mapped to Gene Ontology (GO) categories and counts were computed based on how many genes fell into each category. Statistical significance of enrichment was calculated for each GO term using a hypergeometric distribution function with the set of annotated genes on the Affymetrix chip serving as a background distribution. Multiple testing is adjusted for using a familywise error.

Quantitative Real-Time PCR Validation of Differentially Regulated Genes

Quantitative real-time PCR was performed using ABI Prism Sequence Detection System 5700 (Applied Biosystems, Foster City, CA). RNA samples were treated with DNaseI for 30 min at 37°C, using a DNA-free kit (Ambion, Austin, TX) to eliminate contaminating genomic DNA. First strand cDNA was synthesized from 4 μg of total RNA with random hexamer primers using the SuperScript III first strand synthesis kit (Invitrogen). Fluorogenic primer/probe sets for target genes were purchased from Applied Biosystems as Assays on Demand™ reagents. Specific amplification reactions from the cDNAs were carried out by two-step real time PCR and the relative quantities were obtained by generating a standard curve for each gene. The expression levels of genes were normalized to 18S ribosomal RNA used as internal control. All measurements were performed on triplicate samples. Results of real-time PCR were analyzed by Student's t-test and probability (P) values <0.05 were considered statistically significant.

Bone Marrow Stromal Culture and Staining for Alkaline Phosphatase-Positive Colonies

Total number of progenitors from bone marrow stromal cells (BMSCs), including osteoprogenitors ex vivo, were performed using colony forming unit fibroblast (CFU-f) assay followed by alkaline phosphatase staining. The bone marrow cells were cultured as previously described [Onyia et al., 1998]. Briefly, the diaphyseal middle third of the tibia from individual rats were cut and the marrow was collected by pulse centrifugation and cells were suspended in fresh α-MEM, containing 10% fetal bovine serum (FBS) and 1% penicillin–streptomycin. Cells were counted and plated at a density of 1×10^7 cells per T-75 cm^2 flask. The cells were allowed to adhere for 6 days and then medium was changed for every 2 days. On day 10 the colonies were fixed and stained for alkaline phosphatase using Sigma kit 85L2 (Sigma–Aldrich, St. Louis, MO) as recommended by the manufacturer. Briefly, the cells were fixed in citrate–acetone–formaldehyde fixative (60% citrate-buffered acetone, formaldehyde) for 30 s followed by gentle rinsing with deionized water for 45 s. The colonies were stained with alkaline dye mixture (FAST BLUE RR SALT in 0.25% Naphthol AS-MX phosphate, 0.25% (w/v), pH 8.6) for 15 min at 37°C. The flasks were thoroughly rinsed in deionized water and were allowed to dry at room temperature. The alkaline phosphatase positive colonies are violet colored and were evaluated under microscope. The total number of colonies (CFU-f) were counted and the ratio of alkaline phosphatase positive CFU-f (ALP^+CFU-f) and alkaline phosphatase negative (ALP^-CFU-f) colonies were determined.

Quantitative Image Analysis of Adipocyte Number in the Bone Marrow

Adipocyte number was determined in the tibial sections stained with toluidine blue O. The left tibia (n = 8 animals/group) was excised and fixed in 10% Neutral buffered formalin, decalcified in a hydrochloric acid based solution, processed and embedded in paraffin. Prepared sections were stained with toluidine blue O which stain the cell wall surrounding the adipocyte, so that the adipocytes appear as white holes defined by the blue staining cell wall. Two photographs, using a 10× objective were taken just below the growth plate (metaphyseal region) approximately in the same area on each tibia. The photographs were then

imported into the image analysis program (Image-Pro Plus) and the adipocytes were counted. The number of adipocytes per 10× field was calculated as a percentage of the entire field. Differences between the treatment groups for bone marrow adipocytes were analyzed by Dunnett's test and probability (P) values <0.05 were considered statistically significant.

RESULTS

PTH and GSK-3 Inhibitor (603281-31-8) Increase Bone Mass in Ovx Rats

After treatment for 2 months with PTH, 603281-31-8 or vehicle in Ovx and Sham-operated animal, one femur was analyzed by DXA to validate the anabolic effects of the treatments and the second femur was processed for gene array analysis. As expected, DXA analysis of whole femora, distal femora and midshaft showed significant decreases in BMD of Ovx compared with Sham rats. Ovx for 12 weeks resulted in significantly lower BMD at whole femur and distal femur (10–15%). After treatment with PTH or 603281-31-8 for 2 months, there were significant increases (22%, 36%, and 11 % for PTH; 14%, 15%, and 14% for 603281-31-8) in BMD at the whole femur, distal femur and midshaft, when compared to vehicle-treated Ovx rats ($P < 0.05$). Significant beneficial bone effects of the treatments were observed even in the absence of differences between Sham and Ovx at the midshaft. These effects confirm findings in other experiments where increased histomorphometric indices of bone formation were largely observed with these treatments [Kulkarni et al., 2006; data not shown] (Fig. 1).

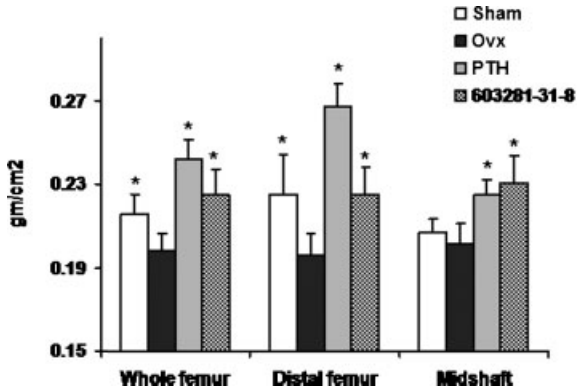

Fig. 1. Femoral bone mineral density as measured by DXA in Sham-operated (Sham) rats treated with vehicle and ovariectomized (Ovx) rats treated with either vehicle, PTH (10 μg/kg/day, s.c.), or 603281-31-8 (3 mg/kg/day, p.o.) for 60 days. At the end of the treatment femoral bone was processed as described in Materials and Methods and density measurements were taken in whole femur, distal femur, and midshaft. Values are expressed as Mean ± SEM (n = 8); *$P < 0.05$ versus Ovx.

Microarray Analysis Identifies Genes Unique and Common to Disease and Treatments

Table I summarizes the results of gene array analysis from mRNA isolated from the distal femur metaphyseal bone. Ovx (when compared to sham control) resulted in altered expression of 1,906 probe sets. Compared to Ovx animals, PTH, and 603281-31-8 treatment regulated 2,416 and 1,508 probe sets, respectively. Figure 2 depicts overlaps of genes in this investigation that were altered by Ovx and the two treatments. Overall, PTH regulated more genes/probe sets and this included 50% of the genes altered by Ovx and 60% of the genes altered by 603281-31-8. Interestingly, a subset of 265 probesets (6.7% of regulated genes) corresponding to 158 non-redundant genes were altered by Ovx and restored or regulated by both PTH and 603281-31-8 (see supplementary Table I for complete gene list). Thus, we focused our investigation on these 158 genes. We hypothesized that a better understanding of this "common set" of genes might reveal the core osteotrophic response such as pathways deregulated in estrogen withdrawal and altered by anabolic treatments. Figure 3 shows a heat map summarizing the expression and regulation of the 158 genes changed with Ovx and altered by treatment with PTH and 603281-31-8, respectively. Overall, 117 genes were upregulated and 41 were down regulated in Ovx animals, compared to sham control. Compared to Ovx, 41 genes and 39 genes were upregulated and 117 and 119 genes were down regulated by PTH and GSK-3 inhibitor treatment, respectively.

To delineate relevant functional or biological processes, we analyzed these 158 common gene

TABLE I. Probe Sets Altered by Ovariectomy and Treatments

Groups	Sham	Ovx	PTH	603281-31-8
Sham	—	1,906	1,120	2,950
Ovx	—	—	2,416	1,508

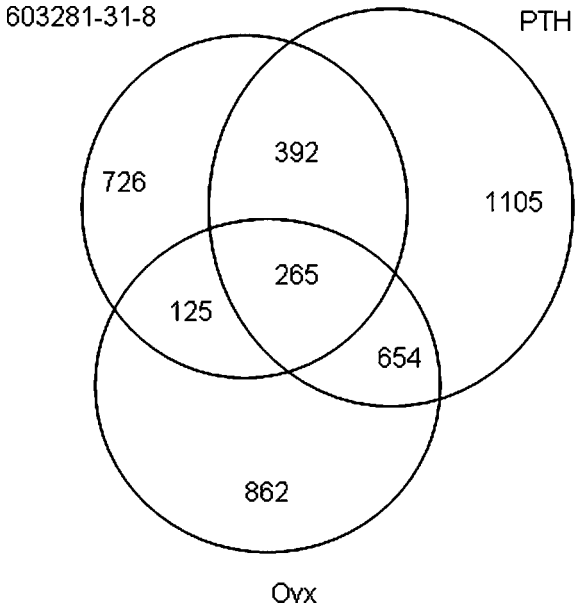

Fig. 2. Venn diagram indicates the number of unique and overlapping genes regulated in distal femur metaphysis of ovariectomized (Ovx) rats and upon treatment with PTH or 603281-31-8.

set using a variety of pathway and annotation tools. Approximately 70% of the genes had reliable annotation and reflect a wide range of pathways and biochemical processes. A notable finding was that over a fourth of the genes on this list are known to have a key role in cartilage or bone metabolism (Table II) and adipogenesis/lipid metabolism (Table III). The genes summarized in Tables II and III became the focus of our current investigation. Follow up of other significantly regulated genes from this analysis will be the subject of a different investigation.

Effect of Ovariectomy and Treatments on Osteogenic, Chondrogenic, and Adipogenic Markers in Bone

A review of the array results did not show changes in the established osteogenic markers such as alkaline phosphatase, biglycan, bone sialoprotein, collagen α_1(I), α_1(V), osteonectin (supplementary Table I) at the analysis stringency used. Examination of the raw data confirms rather subtle changes in these osteogenic markers in both Ovx (disease) and treated groups (data not shown). In contrast, there was a profound effect on chondrogenic and adipogenic/lipid metabolism markers (Tables II and III). To validate our gene array findings, we performed quantitative real-time PCR on some of the osteogenic, chondrogenic, and adipogenic markers in bone. As shown in

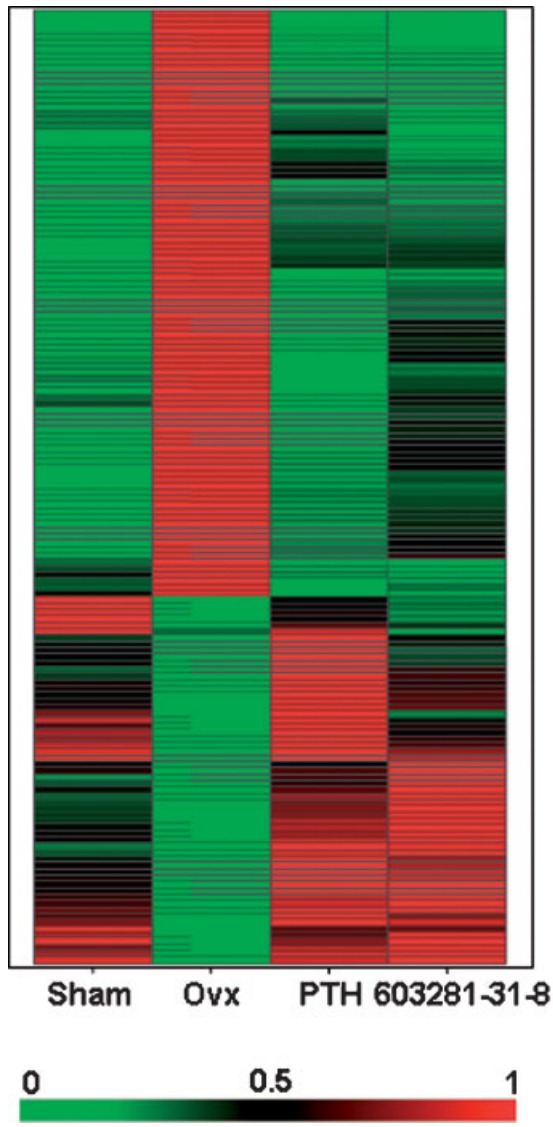

Fig. 3. Heat map of differential gene expression of 158 genes in distal femur metaphysis of rats in disease (Ovx) and following anabolic treatments with PTH and 603281-31-8. Gene expression was obtained using Affymetrix Rat Genome RAE230V2 Gene Chip®. The cluster diagram represents 158 differentially expressed genes with $P < 0.05$ and fold change >1.2. Each row represents a single gene and columns represent control or treatment. Expression levels are colored green for downregulated and red for upregulated genes.

Figure 4A consistent with the array results, ovariectomy marginally decreased the expression levels of bone markers such as alkaline phosphatase, biglycan, bone sialoprotein, collagen α_1(I), α_1(V), osteonectin, procollagen C-proteinase enhancer (PCPE) and runx2. Treatment with GSK-3 inhibitor significantly increased the expression levels of biglycan, collagens and osteonectin, and runx-2, whereas, PTH had no significant effects on these

TABLE II. Genes of Connective Tissue Development and Function Regulated by Ovx and Treatments

ProbeSet	Gene Symbol	Proteome title	Ovx	PTH	603281-31-8
1368836_a_at	Agc1	Aggrecan 1	−2.6	2	1.4
1397360_at	CLECSF1	Cartilage-derived C-type lectin superfamily member 1	−2.3	2.3	1.5
1387767_a_at	Col2a1	Collagen type II, alpha 1	−5.7	3.3	2.6
1373245_at	Col4a1	Collagen type IV, alpha 1	2.4	−1.3	−1.1
1389966_at	Col6a3	Collagen type VI, alpha 3	−1.8	2	1.5
1388973_at	Col9a1	Collagen type IX, alpha 1	−11	3.7	2.9
1377631_at	Col9a3	Procollagen type IX, alpha 3	−5	2.4	1.4
1370944_at	Col10a1	Collagen type X, alpha 1	−8.3	4	2.3
1387137_at	Comp	Cartilage oligomeric matrix protein	−3.5	2.2	1.5
1373803_a_at	Ghr	Growth hormone receptor	2.4	−2.3	−1.6
1370333_a_at	Igf1	Insulin-like growth factor 1	1.4	−1.5	−1.4

markers. As shown in Figure 4B ovariectomy significantly decreased the expression levels of chondrogenic/cartilage markers: aggrecan 1 (Agc1), collagen α_1(II), cartilage-derived retinoic acid sensitive protein (cdrap), cartilage oligomeric matrix protein (COMP), and matrix gla-protein (Mglap), while PTH and GSK-3 inhibitor restored their expression levels to near sham controls. Interestingly, markers of early adipocyte differentiation such as CCAAT/enhancer binding protein, alpha (cebpα), glycerol 3-phosphate dehydrogenase 1 (GPD3), fatty acid binding protein 4 (FABP4), peroxisome proliferators activated receptor gamma (PPARγ), and markers of mature adipocytes and lipid metabolism, lipoprotein lipase (LPL), caveolin, phosphoenolpyruvate carboxykinase (PCK), stearoyl coenzyme-A desaturase 1 (SCD1), 11-beta-hydroxysteroid dehydrogenase type 1 (11β-HSD1), leptin, were significantly increased by ovariectomy; while, PTH and 603281-31-8 treatments decreased or restored their expression levels to sham controls (Fig. 4C). Together, these results suggest a role for bone, cartilage, and adipogenic/lipid metabolism markers in osteopenia and bone anabolic response to PTH and Wnt signaling activation by 603281-31-8.

Ovariectomy Increases Bone Marrow Adiposity but Was Reversed by PTH and 60321-31-8

Given the observed changes in adipocyte and lipid metabolism markers in Ovx and the

TABLE III. Lipid Metabolism Genes Regulated by Ovx and Treatments

ProbeSet	Gene symbol	Proteome title	Ovx	PTH	603281-31-8
1394681_at	AKR1C4	Type 1 3 alpha-hydroxysteroid dehydrogenase	3	−1.9	−1.3
1372111_at	Cav 1	Caveolin 1	1.9	−1.3	−1.5
1377642_at	Cav2	Caveolin 2	3.2	−2	−1.9
1370235_at	Dbi	Diazepam binding inhibitor	1.4	−1.5	−1.3
1368189_at	Dhcr7	7-Dehydrocholesterol reductase	1.4	−1.1	−1.2
1368271_a_at	Fabp4	Fatty acid binding protein 4	3.2	−1.9	−1.3
1371363_at	Gpd3	Gpd3: Glycerol 3-phosphate dehydrogenase 1	3.8	−2.3	−1.7
1386953_at	Hsd11b1	11-Beta-hydroxysteroid dehydrogenase type 1	1.4	−1.7	−1.5
1387132_at	Lipe	Hormone-sensitive lipase	2.5	−1.6	−1.7
1386965_at	Lpl	Lipoprotein lipase	4	−2.2	−1.4
1370949_at	Marcks	Myristoylated alanine-rich protein kinase C substrate	1.3	−1.2	−1.2
1375247_at	Mgll	Monoglyceride lipase	1.2	−1.1	−1.2
1372264_at	Pck1	Phosphoenolpyruvate carboxykinase 1	3.3	−2	−2.5
1393245_at	Phyh	Phytanoyl-CoA hydroxylase	1.2	−1.3	−1.4
1369179_a_at	Pparg	Peroxisome proliferator activated receptor-gamma	1.6	−1.4	−1.4
1370355_at	Scd1	Stearoyl-coenzyme A desaturase 1	8	−2.7	−4.1
1370150_a_at	Thrsp	Thyroid hormone responsive protein	5.2	−2.2	−1.9

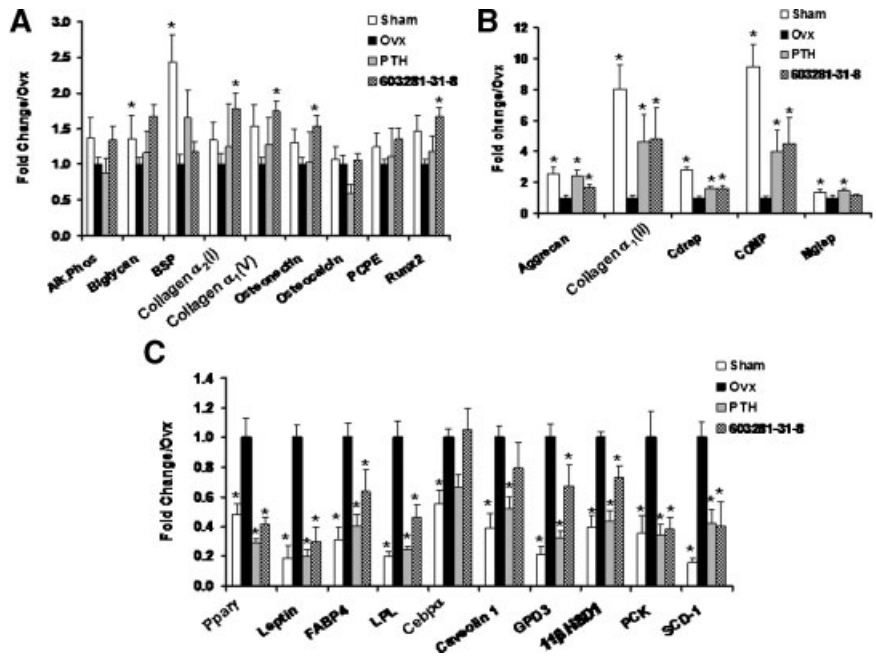

Fig. 4. Effect of PTH and 603281-38-3 on osteogenic, chondrogenic, adipogenic, and lipid metabolism markers. Total RNA was isolated from the distal femur metaphysis 24 h after the last treatment and analyzed by real-time PCR for (**A**) the expression of osteoblast-derived bone formation markers Alk Phos (alkaline phosphatase) biglycan, BSP (bone sialoprotein), collagen α_2 (I), collagen α_1 (V), osteonectin, osteocalcin, procollagen C-proteinase enhancer (PCPE), runx2. **B**: Cartilage-associated markers aggrecan 1, collagen α_1 (II), cartilage-derived retinoic acid sensitive protein (cdrap), cartilage oligomeric matrix protein (COMP), and matrix gla-protein (Mglap). **C**: Adipogenic markers, CCAAT/enhancer binding protein, alpha (cebpα), fatty acid binding protein 4 (FABP4), peroxisome proliferators activated receptor gamma (PPARγ), leptin, lipoprotein lipase (LPL), caveolin, phosphoenolpyruvate carboxykinase (PCK), glycerol 3-phosphate dehydrogenase 1(GPD3), 11-beta-hydroxysteroid dehydrogenase type (11β-HSD1), stearoyl coenzyme-A desaturase 1 (SCD1). Expression was normalized to 18S ribosomal RNA as an internal control. The changes in gene expression are expressed as fold change over Ovx control. The results are expressed as mean ± SEM; $^*P < 0.05$ versus Ovx (n = 8).

treatment groups, we investigated bone marrow adiposity in Ovx and treated animals by quantitative image analysis on histological sections of tibial bone marrow. As shown in Figure 5A osteopenia in Ovx animals was associated with a significant (three-fold) increase in the bone marrow fat as compared to sham controls. Treatment with PTH or 603281-31-8 significantly decreased the amount of marrow fat and restored bone volume as evidenced by the increase in trabecular bone (Fig. 5B). These results suggest that increased expression of markers of adipocytes/lipid metabolism in Ovx animals was consistent with an alteration in the bone marrow fat.

Differential Effects of PTH and 603281-31-8 on the Bone Marrow Progenitors

We evaluated the effect of disease (Ovx), PTH, and 603281-31-8 treatment directly on osteoblastogenesis of bipotential CFU-f marrow stromal cells. We determined number (total CFU-f) and ratio of conversion of osteoprogenitors to osteoblasts (alkaline phosphatase-positive /negative CFU-f colonies) ex vivo as described in Materials and Methods. The numbers of CFU-f colonies were significantly decreased (18%) by Ovx as compared to sham controls (Fig. 6A). Treatment with PTH further decreased CFU-f colonies by 50%, whereas GSK-3 inhibitor increased this to 125% over Ovx controls. However, the ratio of alkaline phosphatase-positive CFU-fs (putative osteoblasts) was significantly decreased by Ovx, whereas treatment with PTH and GSK-3 inhibitor significantly increased these ratios compared to Ovx controls (Fig. 6B).

Effect of Short-Term PTH Treatment on Osteogenic, Chondrogenic, and Adipogenic Markers in Bone

Previous studies confirm at least in part the early effects of Wnt activation on bone formation by decreasing adipogenesis [Bennett et al., 2005]. The results described above were obtained with prolonged treatment of PTH and

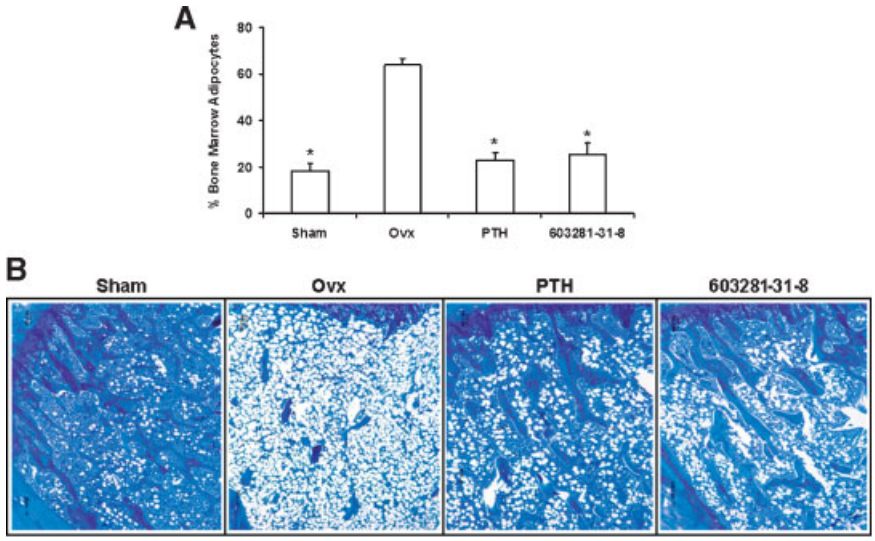

Fig. 5. Quantitative image analysis of histologic sections stained with toluidine blue in the bone marrow of sham, ovariectomized (Ovx) rats treated with PTH or 603281-31-8 in the metaphyseal region of left tibia. Values are represented as means ± SEM (n = 8). Data were analyzed with Dunnett's test. *$P < 0.001$ versus Ovx. The bone marrow adipocytes are visible as white holes. **A**: Percent of bone marrow adipocytes. **B**: Representative histologic sections showing increased marrow fat in Ovx compared to sham control. Please note the decrease in marrow fat accompanied by increase in bone volume after treatment with PTH or 603281-31-8.

GSK-3 inhibitor in Ovx model. To ascertain the short-term effects of intermittent PTH, we evaluated the effects of PTH (once a day treatment for 7 days) on expression levels of osteogenic, chondrogenic, and adipogenic markers. As shown in Figure 7A, PTH significantly increased the expression levels of bone markers; alkaline phosphatase (1.5-fold), biglycan (1.7-fold), bone sialoprotein (1.4-fold), collagen α_1(I) (3.2-fold), α_1(V) (1.9), osteocalcin (3-fold), osteonectin (2.8-fold), PCPE (2.2-fold), and Runx2 (1.6-fold) compared to vehicle controls. No significant change was observed in the expression levels of cartilage-associated markers (Agc1, collagen α_1(II), cdrap, COMP, Mglap) as compared to vehicle controls (Fig. 7B). By contrast, PTH decreased the levels of adipogenic and lipid metabolism markers (cebpα, GPD3, FABP4, Pparγ, LPL, PCK, SCD1, leptin) by 22–56% as compared to vehicle controls (Fig. 7C). These results confirm an early reciprocal effect of PTH on bone i.e., increased osteogenic and decreased adipogenic markers.

DISCUSSION

Underlying this gene array analysis was the search for evidence that there might be any sharing of pathways between PTH and Wnt signaling in their anabolic actions upon the skeleton. In studying the anabolic actions of PTH and 603281-31-8, we specifically focused our efforts on genes commonly regulated by ovariectomy and restored/altered by the treat-

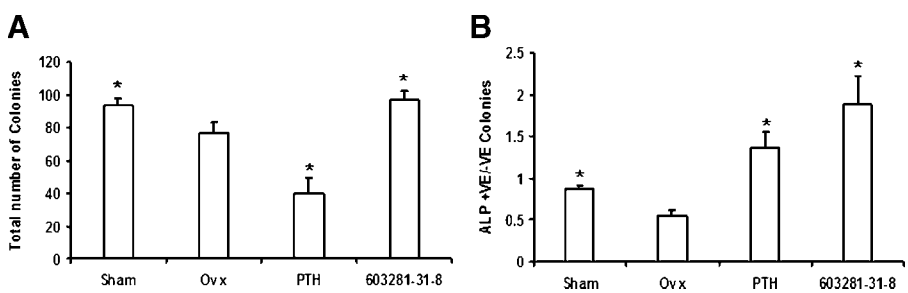

Fig. 6. Effect of Ovariectomy (Ovx), PTH or 603281-31-8 on the number and osteogenic differentiation of bi-potential bone marrow progenitors. Marrow stromal cells were cultured from tibiae of Sham, Ovx, and Ovx rats treated with PTH or 603281-31-8. At the end of the treatment marrow from the tibiae was flushed and the cells were cultured as described in materials and methods. **A**: Total number of CFU-f (colony forming units-fibroblastic). **B**: Ratio of ALP +ve/ALP−ve (alkaline phosphatase-positive to negative) colonies. Values are means ± SEM (n = 8); *$P < 0.05$ versus Ovx.

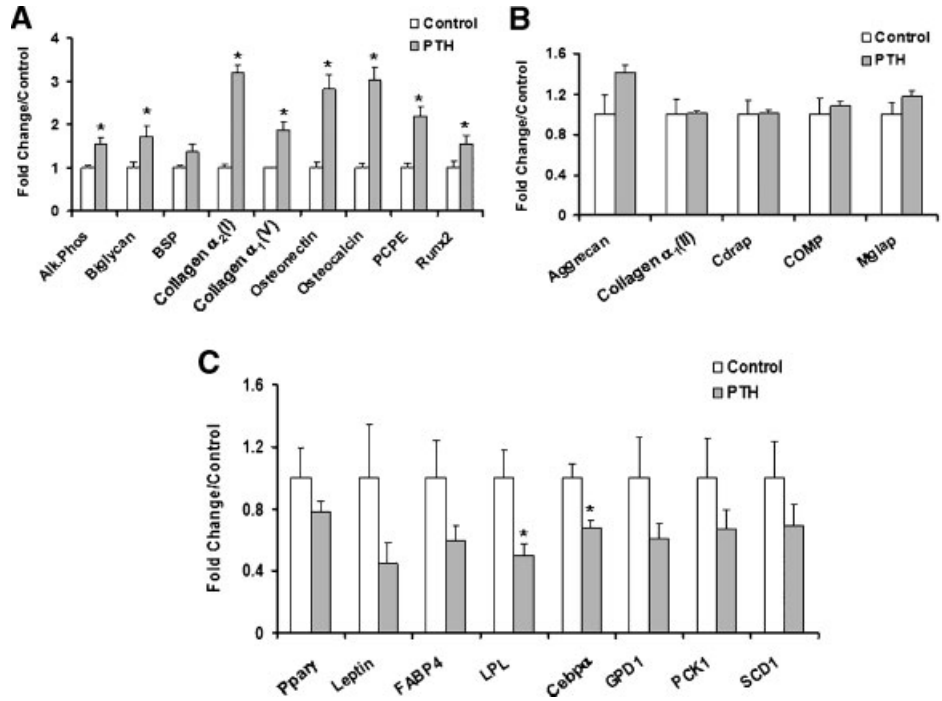

Fig. 7. Effect of short-term PTH treatment on osteogenic, chondrogenic, adipogenic, and lipid metabolism markers. Total RNA was isolated from the distal femur metaphysis 24 h after the last treatment and analyzed by real-time PCR for (**A**) the expression of osteoblast-derived bone formation markers Alk Phos (alkaline phosphatase) biglycan, BSP (bone sialoprotein), collagen α_2 (I), collagen α_1 (V), osteonectin, osteocalcin, PCPE (procollagen C-proteinase enhancer), runx2. **B**: Cartilage-associated markers aggrecan 1, collagen α_1 (II), cartilage-derived retinoic acid sensitive protein (cdrap), cartilage oligomeric matrix protein (COMP), and matrix gla-protein (Mglap). **C**: Adipogenic markers, CCAAT/enhancer binding protein, alpha (cebpα), fatty acid binding protein 4 (FABP4), peroxisome proliferators activated receptor gamma (PPARγ), leptin, lipoprotein lipase (LPL), caveolin, phosphoenolpyruvate carboxykinase (PCK), glycerol 3-phosphate dehydrogenase 1(GPD3), stearoyl coenzyme-A desaturase 1 (SCD1). Expression was normalized to 18S ribosomal RNA as an internal control. The changes in gene expression are expressed as fold change over vehicle controls. The results are expressed as mean ± SEM; $^*P < 0.05$ versus Ovx (n = 5).

ments. These "common marker genes" may be core to the understanding of the bone anabolic actions of PTH and 603281-31-8. We demonstrate that both ovariectomy and the bone anabolic agents regulated the expression levels of osteogenic, chondrogenic, and adipogenic marker genes in rat bone albeit to different magnitude. Based on these results, we suggest that the bone anabolic effects of PTH and 603281-31-8 involve a concerted action on osteoblasts, chondrocytes, and adipocytes of mesenchymal lineages.

In the present study, there was a minimal response of osteogenic markers relative to cartilage-associated and adipogenic markers after long-term treatment with bone anabolics in estrogen-deprived rats. This is in contrast to our previous observation showing short-term treatment regimen with PTH in ovary-intact sexually mature rats, increases the expression levels of osteogenic markers [Onyia et al., 2005]. We confirmed this robust effect on osteogenic markers following short-term PTH treatment (Fig. 7A). This difference in responsiveness can be explained and is consistent with osteoblast differentiation having proceeded throughout the prolonged treatment period in these animals [Trackman, 2005]. It has been noted in vitro that mRNA levels of type I collagen increases during early onset of osteoblast differentiation and diminishes thereafter, followed by matrix maturation and collagen deposition [Hong et al., 2004]. The minimal response of osteogenic markers in this study, to long-term PTH and 603281-31-8 treatment could be attributed to the osteoblast differentiation, matrix maturation and deposition that have occurred. Additionally, the temporal regulation of these markers during different stages of treatments to restore lost bone cannot be excluded and needs further investigation.

Questions arise in this study concerning the role of cartilage-associated markers in bone. We demonstrate the presence and regulation of

cartilage-associated markers such as, type II, IX, and X collagen, aggrecan-1, cdrap, COMP, and Mglap in bone following ovariectomy and altered by 60 days of treatments. While these markers (mRNA) are expressed at appreciable levels, the regulation was not evident in ovary-intact animals after a short course of PTH (24 h after treatment). The expression of these cartilage-associated markers in bone is not likely due to sample contamination from growth plate cartilage, as we carefully removed the growth plate and scraped the underlying subchondral bone surface. Moreover, the consistency and reproducibility in the data argue against such contamination which would be predicted to result in high inter group variability. We have also observed the presence and regulation of these cartilage markers in multiple independent experiments in young (2 weeks to 3 months) and sexually mature rats (6–9 month old rats) so far tested (data not shown). In addition, we have recently confirmed the presence of type II collagen and aggrecan proteins in diaphyseal and metaphyseal region of rat bone using LC-MS profiling and western blot analysis [Schreiweis et al., 2007]. While the significance of these results remains unclear, it calls into question the specificity of these markers in cartilage and the dogma that there are two distinct processes of bone formation; endochondral versus intramembranous. Bone formation by endochondral ossification requires a cartilage template, whereas in the intramembranous process the bone is directly formed from the mesenchyme without a cartilage intermediate. Endochondral and intramembranous ossification have been thought of as independent and distinct processes; however, some evidence indicates the possibility of overlap of these two processes, and that a cartilage intermediate may also occur during intramembranous ossification. Retarded ossification of the calvarial bones was observed in transgenic mice harboring a mutant type II collagen transgene suggesting that type II collagen has an inductive role in intramembranous ossification [Savontaus et al., 2004]. In addition, type II collagen has also been described during fracture healing [Colnot et al., 2004; Ortega et al., 2004; Colnot, 2005]. Recently, the presence and the regulation of cartilage-associated markers (collagen type II and X) have been shown in the bone biopsies of patients with primary hyperparathyroidism [Reppe et al., 2006]. Together, our results showing the expression and regulation of type II collagen along with other cartilage-associated markers by ovariectomy and the anabolic treatments is consistent with their having a role in bone remodeling and bone cell function.

In humans and experimental models of osteopenia (age, ovariectomy, immobilization, glucocorticoid treatment) decrease in bone volume is often associated with an increase in marrow adipose tissue [Meunier et al., 1971; Miniare et al., 1974; Wronski et al., 1986; Burkhhardt et al., 1987; Sottile et al., 2004]. This reciprocity can be explained by the fact that osteoblasts and adipocytes are derived from the same pool of mesenchymal progenitors. Our findings showing an increase in marrow adiposity after Ovx and reversal to sham control levels with PTH and 603281-31-8 is consistent with previous observations in rats and monkeys [Kim et al., 2002; Sato et al., 2004]. Additionally, our results delineate the molecular basis of this effect and precisely link molecular markers to cellular, physiological, and therapeutic outcome by PTH and 603281-31-8. PTH and PTHrP (acting via PTHR1) have empirically been shown to have potent anabolic effects on bone explained largely through effects on osteoblast differentiation and survival. Our in vivo and ex vivo results suggest that this is accompanied by decreased adipogenesis (and perhaps lipogenesis given changes in HSD11β1 and SCD1). This appears to be an early and perhaps important mechanism of PTH action as these were evident with short-term PTH treatment. A recent study [Rickard et al., 2006] suggests that the PTH effects may be mediated via direct inhibitory effect on mesenchymal stem cell differentiation to adipocytes. A previous in vitro study has shown PTHrP can modulate the terminal differentiation of preadipocytes by downregulating PPARγ activity via increased MAPK activity [Chan et al., 2001]. Transgenic mice expressing constitutively active PTH/PTHrP receptors have increased bone formation and CFU-f colonies, accompanied by a delayed formation of yellow marrow with fewer adipocytes in the calcaneum [Kuznetsov et al., 2004]. Similarly, Wnt signaling through the β-catenin-dependent pathway has profound effects on differentiation of mesenchymal progenitors; stimulates osteoblastogenesis and inhibits adipogenesis and regulates other cell fates, including apoptosis [Bennett et al., 2002; Longo et al.,

2004]. Stimulation of Wnt pathway by Wnt3a, LiCl, and GSK-3 inhibitor decreases markers of adipogenesis and increases markers of osteoblast differentiation in pluripotent C3H10T1/2 cells [Jackson et al., 2005; Kulkarni et al., 2006]. In addition, transgenic overexpression of Wnt10B under the FABP4 promoter resulted in increased osteoblastogenesis, bone formation, and decreased adipogenesis [Bennett et al., 2005]. Therefore, the balance between osteoblastogenesis and marrow adipogenesis is a critical thermostat for the maintenance of bone health and a lever in preventing or treating osteopenia. Together, our findings suggest that bone formation by PTH and 603281-31-8 involves an increased osteogenic differentiation of the progenitor cells.

Lastly, the anabolic effect of PTH has been shown to occur via the preferential stimulation of osteoblastic activity over osteoclastic activity. In the present studies, we did not observe an obvious effect of PTH or GSK-3 inhibitor on osteoclast molecular markers such as OPG/RANKL nor did we study osteoclast generation ex-vivo. The effect of PTH on osteoclast generation/actvity is well-documented in vivo and in vitro cultures [Horwood et al., 1998; Murakami et al., 1998; Onyia et al., 2000]. At a molecular level, in rats and mice (ovary-intact), we and other have reported that acute PTH (80 μg/kg) induce a rapid and transient decrease in OPG/RANKL ratio [Onyia et al., 2000]. By contrast, continuous PTH infusion led to rapid but sustained decrease in OPG/RANKL ratio [Ma et al., 2001]. These results suggest a transient and prolonged effect on osteoclast activity/generation in acute and continuous PTH, respectively and are consistent with the many previous studies on the effect of PTH. By contrast, in osteopenic Ovx models (with elevated resorption) the effects of PTH on osteoclast parameters are less well studied. In this Ovx model and under conditions (low dose and long duration of treatment) described in this study, we find by histomophometric analysis that PTH or GSK-3 inhibitor increased largely bone formation parameters with a subtle to non-significant decrease on osteoclast parameters (osteoclast number). Consistent with this was a small to non-significant increase in OPG/RANKL ratio evident by both Taqman and via the gene array results. Key aspects of this finding related to GSK-3 inhibitor effects (and similar with PTH) on resorption were recently communicated (Kulkarni et al., 2006). These results suggest that under these conditions the increased BMD observed with PTH and GSK-3 inhibitor are largely mediated by an increase in bone formation (and decreased adipogenesis) with a subtle effect on resorption.

In summary, we have shown that ovariectomy altered markers of osteogenesis, chondrogenesis, and adipogenesis and these effects were reversed by PTH and GSK-3 inhibitor albeit at different levels. Most exciting is our observation of the presence and alteration of cartilage markers in bone which could suggest a role in bone, perhaps an ongoing biosynthetic turnover of cartilage or progressive bone formation as a result of endochondral or intramembranous ossification. The decrease/inhibition of adipogenesis may be a prerequisite, at least in part, for bone anabolic effects of PTH and GSK-3 inhibitor. The Wnt/β-catenin signaling pathway plays an important role in regulating the fate of many cell types during early development and has also been implicated in bone formation. The differential regulation of these cell types (osteoblast, chondrocytes, and adipocytes) by PTH and GSK-3 inhibitor might be occurring via Wnt pathway and perhaps one of the common pathways through which they stimulate bone formation.

ACKNOWLEDGMENTS

The authors thank Dr. Kannan Thirunavukkarasu for critical review of the manuscript and for valuable suggestions.

REFERENCES

Babich M, Choi H, Johnson RM, King KL, Alford GE, Nissenson RA. 1991. Thrombin and parathyroid hormone mobilize intracellular calcium in rat osteosarcoma cells by distinct pathways. Endocrinology 129:1463–1470.

Babij P, Zhao W, Small C, Kharode Y, Yaworsky PJ, Bouxsein ML, Reddy PS, Bodine PVN, Robinson JA, Bhat B, Marzolf J, Moran RA, Bex F. 2003. High bone mass in mice expressing a mutant LRP5 gene. J Bone Miner Res 18:960–974.

Bellido T, Ali AA, Plotkin LI, Fu Q, Gubrij I, Roberson PK, Weinstein RS, O'Brien CA, Manolagas SC, Jilka RL. 2003. Proteasomal degradation of Runx2 shortens parathyroid hormone-induced anti-apoptotic signaling in osteoblasts. J Biol Chem 278:50259–50272.

Bennett CN, Ross SE, Longo KA, Bajnok L, Hemati N, Johnson KW, Harrison SD, MacDougald OA. 2002. Regulation of Wnt signaling during adipogenesis. J Biol Chem 277:30998–31004.

Bennett CN, Longo KA, Wright WS, Suva LJ, Lane TF, Hankenson KD, MacDougald OA. 2005. Regulation of

osteoblastogenesis and bone mass by Wnt10b. Proc Natl Acad Sci USA 102:3324–3329.

Bollerslev J, Steiniche T, Melsen F, Mosekilde L. 1989. Structural and histomorphometric studies of iliac crest trabecular and cortical bone in autosomal dominant osteopetrosis: A study of two radiological types. Bone 10:19–24.

Bollerslev J, Marks SC, Jr., Pockwinse S, Kassem M, Brixen K, Steiniche T, Mosekilde L. 1993. Ultrastructural investigations of bone resorptive cells in two types of autosomal dominant osteopetrosis. Bone 14:865–869.

Bollerslev J, Ueland T, Grodum E, Haug E, Brixen K, Dipseland O. 1998. Biochemical markers of bone metabolism in benign human osteopetrosis: A study of two types at baseline and during stimulation with triiodothyronine. Eur J of Endocrinol 138:29–35.

Boyden LM, Mao J, Belsky J, Mitzner L, Farhi A, Mitnick MA, Wu D, Insogna K, Lifton RP. 2002. High bone density due to a mutation in LDL-receptor-related protein 5. N Engl J Med 346:1513–1520.

Burkhhardt R, Kettner G, Bohm W, Schmidmeir M, Schlag R, Frisch B, Mallman B, Eisenmenger W, Gilg TH. 1987. changes in trabecular bone, hematopoiesis and bone marrow vessels in aplastic anaemia, primary osteoporosis and old age: A comparative histomorphometric study. Bone 8:157–164.

Chan GK, Deckelbaum RA, Bolivar I, Goltzman D, Karaplis AC. 2001. PTHrP inhibits adipocyte differentiation by down-regulating PPARγ activity via a MAPK-dependent pathway. Endocrinol 142:4900–4909.

Civitelli R, Reid IR, Westbrook S, Avioli LV, Hruska KA. 1988. PTH elevates inositol polyphosphates and diacylglycerol in a rat osteoblast-like cell line. Am J Physiol 255:E660–E667.

Colnot C. 2005. Cellular and molecular interactions regulating skeletogenesis. J Cell Biochem 95:688–697.

Colnot C, Lu C, Hu D, Helms JA. 2004. Distinguishing the contributions of the perichondrium, cartilage, and vascular endothelium to skeletal development. Dev Biol 269:55–69.

Dobnig H, Turner RT. 1995. Evidence that intermittent treatment with parathyroid hormone increases bone formation in adult rats by activation of bone lining cells. Endocrinol 136:3632–3638.

Engler TA, Henry JR, Malhotra S, Cunningham B, Furness K, Brozinick J, Burkholder TP, Clay MP, Clayton J, Diefenbacher C, Hawkins E, Iversen PW, Li Y, Lindstrom TD, Marquart AL, McLean J, Mendel D, Misener E, Briere D, O'Toole JC, Porter WJ, Queener S, Reel JK, Owens RA, Brier RA, Eessalu TE, Wagner JR, Campbell RM, Vaughn R. 2004. Substituted 3-imidazo[1,2-α] pyridine-3-yl-4-(1,2,3,4-tetrahydro-[1,4]diazepino-[6,7,1-*hi*]indol-7-yl)pyrrole-2,5-diones as highly selective and potent inhibitors of glycogen synthase kinase-3. J Med Chem 47:3934–3937.

Glass DA II, Bialek P, Ahn JD, Starbuck M, Patel MS, Clevers H, Taketo MM, Long F, McMahon AP, Lang RA, Karsenty G. 2005. Canonical Wnt signaling in differentiated osteoblasts controls osteoclast differentiation. Dev Cell 8:751–764.

Gong Y, Slee RB, Fukai N, Rawadi G, Roman-Roman S, Reginato AM, Wang H, Cundy T, Glorieux FH, Lev D, Zacharin M, Oexle K, Marcelino J, Suwairi W, Heeger S, Sabatakos G, Apte S, Adkins WN, Allgrove J, Arslan-Kirchner M, Batch JA, Beighton P, Black GCM, Boles RG, Boon LM, Borrone C, Brunner HG, Carle GF, Dallapiccolo B, Paepe AD, Floege B, Halfhide ML, Hall B, Hennekam RC, Hirose T, Jans A, Juppner H, Kim CA, Keppler-Noreuil K, Kohlschuetter A, LaCombe D, Lambert M, Lemyre E, Letteboer T, Peltonen L, Ramesar RS, Romanengo M, Somer H, Steichen-Gersdorf E, Steinman B, Sullivan B, Superti-Furga A, Swoboda W, Boogaard MJV, Hul WV, Vikkula M, Votruba M, Zabel B, Garcia T, Baron R, Olsen BR, Warman ML. 2001. LDL receptor-related protein [5] (LRP5) affects bone accrual and eye development. Cell 107:513–523.

Guo J, Bringhurst FR, Kronenberg HM. 2004. α1 Collagen promoter-directed overexpression of Dkk-1 in mice causes dwarfism and very short limbs. J Bone Miner Res 19 (Suppl 1):S6.

He X, Saint-Jeannet JP, Wang Y, Nathans J, Dawid I, Varmus H. 1997. A member of the Frizzled protein family mediating axis induction by Wnt-5A. Science 275:1652–1654.

Hock JM. 2001. Anabolic actions of PTH in the skeletons of animals. J Musculoskel Neuron Interact 2:1–15.

Holmen SL, Giambernardi TA, Zylstra CR, Buckner-Berghuis BD, Resau JH, Hess JF, Glatt V, Bouxsein ML, Ai M, Warman ML, Williams BO. 2004. Decreased BMD and limb deformities in mice carrying mutations in both Lrp5 and Lrp6. J Bone Miner Res 19:2033–2040.

Holmen SL, Zylstra CR, Mukherjee A, Sigler RE, Faugere MC, Bouxsein ML, Deng L, Clemens TL, Williams BO. 2005. Essential role of β-catenin in postnatal bone acquisition. J Biol Chem 280:21162–21168.

Hong HH, Pischon N, Santana RB, Palamakumbura AH, Chase HB, Gantz D, Guo Y, Uzel MI, Ma D, Trackman PC. 2004. A role for lysyl oxidase regulation in the control of normal collagen deposition in differentiating osteoblast cultures. J Cell Physiol 200:53–62.

Horwood NJ, Elliott J, Martin TJ, Gillespie MT. 1998. Osteotropic agents regulate the expression of osteoclast differentiation factor and osteoprotegerin in osteoblastic stromal cells. Endocrinology 139:4743–4746.

Hsieh JC, Rattner A, Smallwood PM, Nathans J. 1999. Biochemical characterization of Wnt-Frizzled interactions using soluble, biologically active vertebrate Wnt protein. Proc Natl Acad Sci USA 96:3546–3551.

Jackson A, Vayssiere B, Garcia T, Newell W, Baron R, Roman-Roman S, Rawadi G. 2005. Gene array analysis of Wnt-regulated genes in C3H10T1/2 cells. Bone 36:585–598.

Kato M, Patel MS, Levasseur R, Lobov I, Chang BHJ, Glass IIDA, Hartmann C, Li L, Hwang TH, Brayton CF, Lang RA, Karsenty G, Chan L. 2002. Cbfa 1-independent Decrease in osteoblast proliferation, osteopenia, and persistent embryonic eye vascularization in mice deficient in LRP5, a Wnt coreceptor. J Cell Biol 157:303–314.

Kim HJ, Bae YC, Park RW, Choi SW, Cho SH, Choi YS, Lee WJ. 2002. Bone-protecting effect of safflower seeds in ovariectomized rats. Calcif Tissue Int 71:88–94.

Kulkarni NH, Halladay DL, Miles RR, Gilbert LM, Frolik CA, Galvin RJS, Martin TJ, Gillespie MT, Onyia JE. 2005. Effects of parathyroid hormone on Wnt signaling pathway in bone. J Cell Biochem 95:1178–1190.

Kulkarni NH, Onyia JE, Zeng QQ, Tian X, Liu M, Halladay DL, Frolik CA, Engler T, Wei T, Kriauciunas A, Martin TJ, Sato M, Bryant HU, Ma YL. 2006. Orally bioavailable

GSK-3 α/β dual inhibitor increases markers of cellular differentiation in vitro and bone mass in vivo. J Bone Miner Res 21:910–920.

Kuznetsov SA, Riminucci M, Ziran N, Tsutsui TW, Corsi A, Calvi L, Kronenberg HM, Schipani E, Robey PG, Bianco P. 2004. The interplay of osteogenesis and hematopoiesis: Expression of a constitutively active PTH/PTHrP receptor in osteogenic cells perturbs the establishment of hematopoiesis in bone and of skeletal stem cells in the bone marrow. J Cell Biochem 167:1113–1122.

Lacroix CP, Ai M, Chiusaroli R, Morvan F, Roman-Roman S, Vayssiere B, Belleville C, Warman M, Baron R, Rawadi G. 2005. Lrp5-independent activation of Wnt signaling by lithium chloride increases bone formation and bone mass in mice. Proc Natl Acad Sci USA 102:17406–17411.

Little RD, Carulli JP, Del Mestro RG, Dupuis J, Osborne M, Folz C, Manning SP, Swain PM, Zhao SC, Eustace B, Lappe MM, Spitzer L, Zweier S, Braunschweiger K, Benchekroun Y, Hu X, Adair R, Chee L, FitzGerald MG, Tulig C, Caruso A, Tzellas N, Bawa A, Franklin B, McGuire S, Nogues X, Gong G, Allen KM, Anisowicz A, Morales AJ, Lomedico PT, Recker SM, Eerdewegh PV, Recker RR, Johnson ML. 2002. A mutation in the LDL receptor-related protein 5 gene results in the autosomal dominant high-bone-mass trait. Am J Hum Genet 70: 11–19.

Longo KA, Wright WS, Kang S, Gerin I, Chiang SH, Lucas PC, Opp MR, MacDougald OA. 2004. Wnt10b inhibits development of white and brown adipose tissues. J Biol Chem 279:35503–35509.

Ma YL, Cain RL, Halladay DL, Yang X, Zeng Q, Miles RR, Chandrasekhar S, Martin TJ, Onyia JE. 2001. Catabolic effects of continuous human PTH (1-38) in vivo is associated with sustained stimulation of RANKL and inhibition of osteoprotegerin and gene-associated bone formation. Endocrinology 142:4047–4054.

Mao J, Wang J, Liu B, Pan W, Farr IIIGH, Flynn C, Yuan H, Takada S, Kimelman D, Li L, Wu D. 2001a. Low-density lipoprotein receptor-related protein-5 binds to axin and regulates the canonical Wnt signaling pathway. Mol Cell 7:801–809.

Mao B, Wu W, Li Y, Hoppe D, Stannek P, Glinka A, Niehrs C. 2001b. LDL-receptor- related protein 6 is a receptor for Dickkopf proteins. Nature 411:321–325.

McClelland P, Onyia JE, Miles R, Tu Y, Liang J, Harvey AK, Chandrasekhar S, Hock J, Bidwell JP. 1998. Intermittent administration of parathyroid hormone (1-34) stimulates matrix metalloproteinase-9 (MMP-9) expression in long bone. J Cell Biochem 70:391–401.

Meunier P, Aaron J, Edouard C, Vignon G. 1971. Osteoporosis and the replacement of cell populations of the marrow by adipose tissue. A quantitative study of 84 iliac bone biopsies. Clin Orthop 80:147–154.

Miles RR, Sluka JP, Halladay DL, Santerre RF, Hale LV, Bloem L, Boguslawski G, Thirunavukkarasu K, Hock JM, Onyia JE. 2000a. Dynamic regulation of RGS2 in bone: Potential new insights into parathyroid hormone signaling mechanisms. Endocrinol 141:28–36.

Miles RR, Sluka JP, Halladay DL, Santerre RF, Hale LV, Bloem L, Thirunavukkarasu K, Galvin RJS, Hock JM, Onyia JE. 2000b. ADAMTS-1: A cellular disintegrin and metalloprotease with thrombospondin motifs is a target for parathyroid hormone. Endocrinol 141:4533–4542.

Miles RR, Sluka JP, Halladay DL, Santerre RF, Hale LV, Bloem L, Patanjali SR, Galvin RJ, Ma L, Hock JM, Onyia JE. 2002. Parathyroid hormone (hPTH 1-38) stimulates the expression of UBP41, an ubiquitin-specific protease, in bone. J Cell Biochem 85:229–242.

Miniare P, Meunier PJ, Edouard C, Bernard J, Courpron J, Bourett J. 1974. Quantitative histological data on disuse osteoporosis. Calcif Tissue Res 17:57–73.

Murakami T, Yamamoto M, Ono K, Nishikawa M, Nagata N, Motoyoshi K, Akatsu T. 1998. Transforming growth factor-beta1 increases mRNA levels of osteoclastogenesis inhibitory factor in osteoblastic/stromal cells and inhibits the survival of murine osteoclast-like cells. Biochem Biophys Res Commun 252:747–752.

Neer RM, Arnaud CD, Zanchetta JR, Prince R, Gaich GA, Reginster JY, Hodsman AB, Eriksen EF, Ish-Shalom S, Genant HK, Wang O, Mitlak BH. 2001. Effect of parathyroid hormone (1-34) on fractures and bone mineral density in postmenopausal women with osteoporosis. N Engl J Med 344:1434–1441.

Onyia JE, Bidwell J, Herring J, Hullman J, Hock JM. 1995. In vivo, human parathyroid hormone fragment (hPTH 1-34) transiently stimulates immediate early response gene expression, but not proliferation, in trabecular bone cells of young rats. Bone 17:479–484.

Onyia JE, Miller B, Hulman J, Liang J, Galvin R, Frolik C, Chandrasekhar S, Harvey AK, Bidwell J, Herring J, Hock JM. 1997. Proliferating cells in the primary spongiosa express osteoblastic phenotype in vitro. Bone 20:93–100.

Onyia JE, Clapp DW, Long H, Hock JM. 1998. Osteoprogenitor cells as targets for ex vivo gene transfer. J Bone Miner Res 13:20–30.

Onyia JE, Miles RR, Yang X, Halladay DL, Hale J, Glasebrook A, McClure D, Seno G, Churgay L, Chandrasekhar S, Martin TJ. 2000. In vivo demonstration that human parathyroid hormone 1-38inhibits the expression of osteoprotegerin in bone with the kinetics of an immediate early gene. J Bone Miner Res 15:863–871.

Onyia JE, Helvering LM, Gelbert L, Wei T, Huang S, Chen P, Dow ER, Maran A, Zhang M, Lotinun S, Lin X, Halladay DL, Miles RR, Kulkarni NH, Ambrose EM, Ma YL, Frolik CA, Sato M, Bryant HU, Turner RT. 2005. Molecular profile of catabolic versus anabolic treatment regimens of parathyroid hormone (PTH) in rat bone: An analysis by DNA microarray. J Cell Biochem 95:403–418.

Ortega N, Behonick DJ, Werb Z. 2004. Matrix remodeling during endochondral ossification. Trends in Cell Biol 14:86–93.

Pinson KI, Brennan J, Monkley S, Avery BJ, Skarnes WC. 2000. An LDL-receptor-related protein mediates Wnt signaling in mice. Nature 407:535–538.

Radeff M, Singh ATK, Stern PH. 2004. Role of protein kinase A, phospholipase C and phospholipase D in parathyroid hormone receptor regulation of protein kinase Cα and interleukin-6 in UMR-106 osteoblastic cells. Cell Signal 16:105–114.

Reppe S, Stilgren L, Olstad OK, Brixen K, Nissen-Meyer LS, Gautvik KM, Abrahamsen B. 2006. Gene expression profiles give insight into the molecular pathology of bone in primary hyperparathyroidism. Bone 39:189–198.

Rickard DJ, Wang FL, Rodriguez-Rojas AM, Wu Z, Trice WJ, Hoffman SJ, Votta B, Stroup GB, Kumar S, Nuttall ME. 2006. Intermittent treatment with parathyroid hormone (PTH) as well as a non-peptide small molecule agonist of the PTH1 receptor inhibits adipocyte differentiation in human bone marrow stromal cells. Bone 39:1361–1372.

Rixon RH, Whitfield JF, Gagnon L, Isaacs RJ, Maclean S, Chakravarthy B, Durkin JP, Neugebauer W, Ross V, Sung W, Willick GE. 1994. Parathyroid hormone fragments may stimulate bone growth in ovariectomized rats by activating adenylyl cyclase. J Bone Miner Res 9:1179–1189.

Rosen CJ, Bilezikian JP. 2001. Clinical review 123: Anabolic therapy for osteoporosis. J Clin Endocrinol Metabol 86:957–964.

Sato M, Westmore M, Ma YL, Schmidt A, Zeng QQ, Glass EV, Vahle J, Brommage R, Jerome CP, Turner CH. 2004. Teriparatide [PTH(1-34)] strengthens the proximal femur of ovariectomized nonhuman primates despite increasing porosity. J Bone Miner Res 19:623–629.

Savontaus M, Rintala-Jamsa M, Morko J, Ronning O, Metsaranta M, Vuorio E. 2004. Abnormal craniofacial development and expression patterns of extracellular matrix components in transgenic Del1 mice harboring a deletion mutation in the type II collagen gene. Orthod Craniofacial Res 7:216–226.

Schreiweis MA, Butler JP, Kulkarni NH, Knierman MD, Higgs RE, Halladay DL, Onyia JE, Hale JE. 2007. A proteomic analysis of adult rat bone reveals the presence of cartilage/chondrocyte markers. J Cell Biochem 101: 466–476.

Scott DK, Brakenhoff KD, Clohisy JC, Quinn CO, Partridge NC. 1992. Parathyroid hormone induces transcription of collagenase in rat osteoblastic cells by a mechanism utilizing cAMP and requiring protein synthesis. Mol Endocrinol 6:2153–2159.

Slusarski DC, Corces VG, Moon RT. 1997. Interaction of Wnt and a Frizzled homologue triggers G-protein-linked phosphatidylinositol signalling. Nature 390:410–413.

Sottile V, Seuwen K, Kneissel M. 2004. Enhanced bone marrow adipogenesis and bone resorption in estrogen-deprived rats treated with the PPARgamma agonist BRL49653(Rosiglitazone). Calcif Tissue Int 75:329–337.

Tobimatsu T, Kaji H, Sowa H, Naito J, Canaff L, Hendy GN, Sugimoto T, Chihara K. 2006. Parathyroid hormone increases β-catenin levels through Smad3 in mouse osteoblastic cells. Endocrinol 147:2583–2590.

Trackman PC. 2005. Diverse biological functions of extracellular collagen processing enzymes. J Cell Biochem 96:927–937.

Uusitalo M, Heikkila M, Vainio S. 1999. Molecular genetic studies of Wnt signaling in the mouse. Exp Cell Res 253:336–348.

Wang YK, Samos CH, Peoples R, Perez-Jurado LA, Nusse R, Francke U. 1997. A novel human homologue of the Drosophila frizzled Wnt receptor gene binds wingless protein and is in the Williams syndrome deletion at 17q11.23. Hum Mol Genet 6:465–472.

Wang FS, Lin CL, Chen YJ, Wang CJ, Yang KD, Huang YT, Sun YC, Huang HC. 2005. Secreted frizzled-related protein 1 modulates glucocorticoid attenuation of osteogenic activities and bone mass. Endocrinol. 146:2415–2423.

Wesenbeeck LV, Cleiren E, Gram J, Beals RK, Benichou O, Scopelliti D, Key L, Renton T, Bartels C, Gong Y, Warman ML, Varnejoul MCD, Bollerslev J, Hul WV. 2003. Six novel missense mutations in the LDL receptor-related protein 5 (LRP5) gene in different conditions with an increased bone density. Am J Hum Genet 72:763–771.

Westendorf JJ, Kahler RA, Schroeder TM. 2004. Wnt signaling in osteoblasts and bone diseases. Gene 341: 19–39.

Wodarz A, Nusse R. 1998. Mechanism of Wnt signaling in development. Annu Rev Cell Dev Biol 14:59–89.

Wronski TJ, Walsh CC, Ignaszewski LA. 1986. Histological evidence for osteopenia and increased bone turnover in ovariectomized rats. Bone 7:119–123.

Yang-Snyder J, Miller JR, Brown JD, Lai C, Moon RT. 1996. A frizzled homolog functions in a vertebrate Wnt signaling pathway. Curr Biol 6:1302–1306.